Final Technical Report

NASA - Ames Research Center

NASA-Ames Award No. NAG 2 - 484, ~~Supplement 2.~~

Reduction in Size and Unsteadiness of a VTOL Ground Vortex by Ground Fences

Co-Principal Investigators: John M. Cimbala and Michael L. Billet

The Pennsylvania State University, University Park, Pennsylvania 16802

and

Graduate Assistant: Todd B. Harman

Present address: 5284 Cobble Creek Rd., Apt. 13J, Salt Lake City, UT 84117

April 15, 1993

Abstract

A ground vortex, produced when a jet impinges on the ground in the presence of crossflow, is encountered by V/STOL aircraft hovering near the ground, and is known to be hazardous to the aircraft. The objective of this research was to identify a ground-based technique by which both the mean size and fluctuation in size of the ground vortex could be reduced. A simple passive method has been identified and examined in the laboratory. Specifically, one or two fine wire mesh screens (ground fences), bent in a horseshoe shape, located on the ground in front of the jet impingement point, proved to be very effective. The ground fences work by decreasing the momentum of the upstream-traveling wall jet, causing an *effectively* higher freestream-to-jet velocity ratio (V_∞/V_j), and thus a ground vortex smaller in size and unsteadiness. At $V_\infty/V_j = 0.15$, the addition of a single ground fence resulted in a 70% reduction in mean size of the ground vortex. With two ground fences, the mean size decreased by about 85%. Fluctuations in size decreased nearly in proportion to the mean size, for both the single and double fence configurations. These results were consistent over a wide range of jet Reynolds number ($10^4 < Re_{jet} < 10^5$); further development and full-scale Reynolds number testing are required, however, to determine if this technique can be made practical for the case of actual VTOL aircraft.

Nomenclature

A	Cross-sectional area of a slice through the centerline of the ground vortex.
d_j	Inner diameter of jet.
h	Distance from the nozzle exit plane to the ground plane.
h_v	Ground vortex height (from ground to top of ground vortex).
Re_{jet}	Jet Reynolds number based on diameter ($Re_{jet}=V_j d_j/\nu$).
V_j	Velocity of jet at nozzle exit.
V_∞	Freestream velocity, (also referred to as crossflow velocity).
x	Distance along ground plane, in the direction upstream of the jet centerline.
y	Distance normal to the ground plane.
z	Distance along ground plane, perpendicular to the freestream.
ν	Kinematic viscosity.

Introduction

When a circular jet impinges on the ground, with a crossflow present, a horseshoe shaped ground vortex forms upstream of the jet impingement point. The ground vortex has large fluctuations in size (unsteadiness), and is of appreciable concern to V/STOL aircraft pilots and designers. This phenomenon can be encountered when there is either relative motion between the aircraft and the landing zone during short takeoffs and landings, or in hover and vertical takeoffs and landings when a naturally occurring cross wind is present. If operating over loose terrain, the unsteady ground vortex can create a dust cloud that can be re-ingested in the engine inlet causing foreign object damage to the high pressure compressor[1]. It also induces forces and moments on the aircraft and can lead to ingestion of heated exhaust air into the engine inlet, causing thrust loss or engine failure.

The formation of the ground vortex is as follows. First, a turbulent jet exits vertically from a circular nozzle, and impinges on the ground. At the impingement point the jet spreads out nearly uniformly over 360° and proceeds along the ground, producing a radially developing wall jet velocity profile. A portion of the wall jet encounters the crossflow, caused by relative motion or a cross wind, and this reduces the wall jet's momentum. The wall jet's momentum continues to decrease until the crossflow forces it to roll back upon itself. Entrainment from the jet forces the now reversed flow down into the wall jet, thus creating the roll up of the ground vortex. A schematic diagram of the vortex can be found in Figure 1, which is a horizontal side view; if viewed from the top, the axis of the ground vortex would be seen to curve around and turn downstream in a horseshoe shape.

Extensive experimental and numerical studies have been performed on the physical characteristics of the ground vortex. Summaries of recent research can be found in NASA-Ames Ground Vortex Workshops held in 1985 and 1987[2,3], in the Society of Automotive Engineers (SAE) Powered Lift Conference in 1987[4], and in the 1989 SAE Aerotech Conference[5]. Of particular interest is work done by Cimbala et al.[6] and Gaublomme[7] in which the issue of unsteadiness was addressed. Through the use of hot-wire anemometry and high speed photography with smoke wires, they discovered that the ground vortex had a characteristic "puffing" frequency. Their flow visualization revealed severe fluctuations in the

height of the ground vortex. The flow field was very unsteady, especially at low values of V_∞/V_j, as can be seen in Figure 2, taken from Cimbala et al.[6]. At larger values of V_∞/V_j the height of the ground vortex, as well as the unsteadiness in height, decreased significantly. For example, at $V_\infty/V_j = 0.05$ the vortex height (h_V) varied from about 3 to nearly 9 jet diameters, while at $V_\infty/V_j = 0.15$, h_V/d_j varied from about 2.5 to 4. Although some work has been done on characterizing the unsteadiness, little research has gone into reducing or controlling the mean size and fluctuations in size of the ground vortex; this was the objective of the present study.

Experimental Setup and Instrumentation

Low Reynolds Number Tests

Low Reynolds number experiments were performed in a water channel. The channel test section, which had dimensions of 152 x 152 x 457 mm (6 x 6 x 18 in.), was made of clear Plexiglas for flow visualization, and had a velocity range of 0.03 to 0.76 m/s (0.1 to 2.5 ft/s.). The top of the test section was fitted with a removable cover, with the jet mounted perpendicular to it along the test section centerline ($z = 0$). The coordinate system and relevant dimensions used are shown in Figure 1. Further details about the instrumentation can be found in Harman[8].

Flow visualization was provided via an Argon-ion 1300 mW laser and minute amounts of fluorescing dye in the jet. The laser beam passed through a cylindrical glass rod that dispersed the beam into a sheet of light. The orientation of the sheet could be varied, enabling any "slice" of the ground vortex to be visualized. Videos and still pictures were taken while the sheet was positioned parallel to the freestream at the tunnel centerline ($z = 0$). This gave excellent visualization of a cross section of the jet and the most forward portion of the ground vortex.

The jet issued from a 380 mm (15 in.) long brass tube, with an exit diameter that was reduced in stepwise fashion to 5.68 mm (0.224 in.). The exit plane of the jet was mounted 17 mm above the ground plane, and the freestream and jet velocities were set at 0.27 m/s (Re_{jet} = 8,900) and 1.8 m/s respectively.

For all cases in the present study, the velocity ratio ($V_\infty/V_j = 0.15$) and nondimensional jet height ($h/d_j=3.0$) were the same as those of previous studies by Cimbala et al.[6]. The jet diameter and velocity were chosen to minimize vortex leg-channel wall interference. This was verified by orienting the light sheet to illuminate the vortex legs.

The fences used were made of a fine (100 x 100 mesh) 30.3% porosity screen, 0.5 times d_j in height, bent in a horseshoe shape, and supported at the top with a small rod frame. The double ground fence consisted of two screens, each 0.5 d_j high, that were separated by 0.5 d_j. A typical location of the ground fence has been sketched in Figure 1.

Still photographs were taken with a Nikon F2 35-mm camera with a 50-mm Nikkor lens and a Promaster Spectrum magnifier lens +4. The shutter speed was 1/2000 of a second, and Kodak Tmax-400 black and white film was used. Videos were taken with a Sony Handycam Pro 8 mm camera with a Sony Teleconversion lens (+4), at a rate of 30 frames per second, with a shutter speed of 1/2000 sec. Bioscan Optimas v 3.10 image processing software was used on an IBM compatible 386 personal computer with a PCvision Plus 640 x 512, 8 bit frame grabber. Two Burle black and white monitors were connected to the image processor, and playback of the videos was done with the Handycam. Calibration of the image processor was done with videos of a marked ruler, taken prior to the test runs.

The video images consisted of a cross section of the impinging jet, and the forward most portion of the ground vortex. The image processor could capture individual frames from the video, filter them, outline the vortex, and calculate the area of the outlined region. The variation of cross-sectional area in time was used as a measurement of the fluctuations in size of the ground vortex. This provided a more global measurement of size fluctuations than did the simple linear measurement of h_v (as in Figure 2). (Note however that h_v is probably of more significance to an actual aircraft when concerned with hot gas re ingestion.) After a number of frames were processed, the mean area and rms fluctuation in area were calculated. This technique was used to compare the ground vortex under the single, double, and no fence conditions.

To keep uniformity and to expedite the processing of multiple frames, a macro program was written, which instructed the software to acquire an image, apply a region of interest (ROI) to the frame, filter the ROI, draw an outline of the ground vortex, and calculate the cross-sectional area of the ground vortex. The filter used was an average 5 x 5 convolution filter. Border detection (threshold) was set by examining a circular object of known area with the image processor, and adjusting the threshold until the processed area equaled the actual area. To ensure consistency, this setting, along with the brightness and contrast, were held constant throughout *all* of the image processing. After the threshold was set the macro was used to rapidly process individual frames of the vortex, with each frame being checked visually for the accuracy of the outline. Note that the ROI, for all of the test cases, was placed so that the jet was not included in the area calculation. The fences produced shadows in the vortex core, resulting in computer - calculated areas that were lower than the actual values. To adjust for this, correction factors were added to the data. For the single fence case, the fence produced a shadow of nearly constant area. This was measured separately from 10 randomly chosen video frames, averaged, and added to the data. For the double fence, the exact correction factor could not be defined; instead, a maximum and a minimum area were calculated for each frame. The maximum area (referred to as the *corrected* area) was calculated by assuming that the light from the vortex completely surrounded the fence, and a well defined shadow resulted; the shadow area was measured and added to the data. The minimum area, or uncorrected area, assumed no shadow was produced; therefore no correction was added to the data. This produced a range of possible results for the double fence case, the actual area falling somewhere in between these two extremes.

High Reynolds Number Tests

High Reynolds number tests were conducted in the 48-inch, octagonal, closed-circuit wind tunnel at ARL/Penn State. This was the same facility as used by Cimbala et al.[6] in the previous tests. A 4 ft. x 8 ft. ground board and jet board were mounted horizontally in the wind tunnel, with the jet board slightly angled to give a zero pressure gradient throughout the test section. The jet was mounted vertically, impinged against the ground board, and was driven by a variable speed blower. The jet diameter was 38.1 mm (1.5 in.) with the exit plane of the jet 114 mm (4.5 in., $h/d_j = 3.0$) above the ground board. The

freestream velocity (V_∞) was 6.9 m/s (22.5 ft/s), and the jet velocity (V_j) was 45.7 m/s (150 ft/s), which corresponds to $V_\infty/V_j = 0.15$. Details about instrumentation can be found in Harman[8].

To provide flow visualization, the centerline of the flow field was illuminated by light that passed vertically through a thin streamwise Plexiglas slit in the ground board. Smoke from an industrial strength smoke bomb (Superior #3C, 1A) was injected near the blower exit, passed through the plenum chamber, and exited the jet. Light from a Pallite VII, positioned outside of the wind tunnel, passed through the slit and formed a light sheet similar to the laser light sheet of the water channel studies. The results were documented with a Panasonic WV 3400 VHS video camera that had a film speed of 30 frames per second.

Results

Low Reynolds Number Tests

Preliminary experiments were performed in the low speed water channel to explore several different techniques for controlling the ground vortex associated with a single circular jet impinging perpendicular to the ground in a crossflow. Details about these preliminary experiments can be found in the Masters thesis of Harman[8]. These studies showed that disturbances in the freestream, freestream boundary layer, and jet had little impact on the size and unsteadiness of the vortex. However, the addition of roughness, or the placement of horseshoe shaped trip wires in the wall jet region altered the size of the vortex significantly. This led to the hypothesis that placement of fine mesh screens in the wall jet would break up large scale structures and decrease the momentum of the wall jet, thus reducing both the size and unsteadiness of the ground vortex. The following is a description of several experiments performed using the ground fence(s), the quantitative method of examining the ground vortex, and the results of the study.

Two video images of the unmodified ground vortex at $Re_{jet} = 8{,}900$ are shown in Figure 3. The image of Figure 3b has been image processed; the applied region of interest and the outline of the ground vortex (as calculated by the computer) are shown. The video images were taken at different times, but under identical flow conditions, and illustrate the mean size and variation in size of the ground vortex. The

large variation in height h_v of the ground vortex is quite apparent in these images, illustrating the unsteadiness associated with such a flow. In fact, analysis of hundreds of video frames similar to those shown in Figure 3 yielded a range of $3.2 < h_v/d_j < 7.2$, which is significantly greater than the range reported by Cimbala et al.[6] at a higher Reynolds number (120,000). It is not known whether this discrepancy is due to Reynolds number effects or some other reason(s). The range for the present data, which was calculated only at $V_\infty/V_j = 0.15$, has also been plotted on Figure 2 for comparison.

The effect of the single fence at various streamwise locations (x/d_j = 1.0, 2.0, and 3.0) is shown in Figure 4. These pictures are still photographs of a "typical" ground vortex. For each case, the mean size of the ground vortex was reduced considerably compared to that of the unmodified flow of Figure 3. The effectiveness of the fence was dependent on its streamwise location, as seen in Figure 4. For example, the fence when located at $x/d_j = 2.0$ was more effective at reducing the size of the ground vortex than when located at either $x/d_j = 1.0$ or 3.0.

Figure 5 shows still photographs of the double fence on the ground plane at streamwise locations x/d_j = 0.5, 2.0, and 3.0. From the figure it is clear that the mean size of the ground vortex was dramatically reduced compared to the unmodified case in Figure 3 or the single fence cases of Figure 4. In addition, the streamwise location of the double fence affected the size and location of the ground vortex. Optimization of fence location, mesh size, etc. was not attempted in these studies. Instead, a fence location of $x/d_j = 2.0$ was chosen for quantitative study. Note that for the case of the double fence, the streamwise location refers to the location of the fence *nearest* the jet impingement point.

For quantitative analysis, video images were examined frame by frame according to the technique described above. Approximately ten seconds of video (300 frames) were analyzed for each configuration: no fence, single fence at $x/d_j = 2.0$, and double fence at $x/d_j = 2.0$. For each frame, the centerline cross-sectional area of the ground vortex was calculated; this is plotted in Figure 6 for all three configurations as a function of time. The effect of the fences is clear—a decrease in both mean size and unsteadiness of the ground vortex. Table 1 re-illustrates this point; the single fence reduced the mean size by about 70%, and the double fence by approximately 84-90%. Also shown in the table is the rms value of the fluctuations

about the mean area for each case, a measure of the unsteadiness of the cross-sectional area. The unsteadiness is reduced nearly in proportion to the reduction of mean cross-sectional area. Figure 7 is a summary figure that illustrates the maximum and minimum cross-sectional area of the ground vortex, taken from the videos. The effect of the single and double fence is evident.

Table 1. Summary of area results for the unmodified, single, and double fence configurations.

Description	Mean cross-sectional area (mm^2)	Uncertainty in area measurement	Range of reduction in mean size	RMS fluctuation in area (mm^2)
No fence	440	- 4% , +2%	—	81
Single fence	140	-12% , +0%	67-72%	23
Double fence (uncorrected)	49	-13% , +0%	88-90%	7.5
Double fence (corrected)	66	-13% , +0%	84-87%	7.5

High Reynolds Number Tests

Figure 8 shows a smoke filled jet in a wind tunnel crossflow, flowing from right to left, at a higher jet Reynolds number, Re_{jet} = 97,000. The unmodified, single, and double fence configurations are shown, and represent the maximum size of the ground vortex from ten seconds of video. This figure illustrates the reduction in size of the ground vortex when under the influence of the fences and agrees qualitatively with the results of the low Reynolds number studies. The poor visualization, when compared to the previous studies, is the result of a higher jet Reynolds number, a slow camera shutter, and the working medium being air rather than water. No attempts at quantifying these flow visualizations were made.

Error Discussion

The image processor outlined a region which did not have a well defined border, and this produced a significant amount of uncertainty. For consistency, a threshold setting was chosen based on a video image of a circular object of known area. When applied to the ground vortex images, this threshold setting proved to be slightly higher than if set manually. This ensured that all of the vortex as well as some of the surrounding noise (gray areas), were included in the outline, which biased all of the results. This method was used *consistently* for the no, single, and double fence configurations. The degree of uncertainty was impossible to calculate since the exact area of the vortex at any specific time was not known. Instead a pseudo percent uncertainty was calculated by comparing the constant threshold areas to manual threshold areas for 10 frames of data for each configuration. The biasing of the results is shown in the negative percent uncertainty in Table 1. It should be noted that the increase in uncertainty of the single and double fence cases can be attributed to the decrease in resolution due to the smaller size of the vortex. The camera was at a fixed position, with constant settings, for all three cases for consistency.

Discussion and Conclusions

The ground vortex produced by a single circular jet impinging perpendicular to the ground in a crossflow has been experimentally studied. A passive method for reducing the mean size and unsteadiness has been found, namely placement of single or double fine screen fences, bent in a horseshoe shape in the wall jet. This method has been examined at a low jet Reynolds number in a recirculating water channel, and also at a higher Reynolds number in a wind tunnel. Flow visualization was used extensively to show the effect of the fences qualitatively. Quantitative analysis was performed with an image processor at the lower jet Reynolds number. From these investigations the following conclusions can be made:

1. Single and double fine mesh fences placed in the wall jet region dramatically reduced the mean and fluctuating size of the ground vortex. The effect of the fence(s) was consistent over a wide range of jet

Reynolds number ($8{,}900 < Re_{jet} < 97{,}000$).

2. The ground fences reduced the wall jet's momentum and caused an *effectively* higher freestream-to-jet velocity ratio V_∞/V_j (by reducing the effective V_j). Essentially, the fences moved the flow regime to the right in Figure 2, where both the size of the ground vortex and fluctuations in size are smaller.

No attempt has been made to optimize the fences for ground vortex suppression. The authors recommend that full-scale studies be performed on a hovering VTOL aircraft in crossflow. Modifications of a landing pad by the addition of fences would be required to verify the effectiveness. If proven feasible, optimization studies could be conducted. Mesh size, fence height, number of fences, and streamwise location are some of the parameters which need to be optimized. Other means of reducing the wall jet momentum should also be considered. Note that the device(s) for reducing the wall jet momentum will have to stand up under the temperature and pressure of the jet exhaust, yet also permit the aircraft to taxi over them with damage to neither the aircraft nor the device. The devices would also need to be omnidirectional (perhaps circular?) due to changing wind direction. It is not clear whether this technique will ever be practical for routine operation with full-scale aircraft, perhaps only under certain specific operating conditions. The primary advantage is that the addition of ground fences or other devices *on the ground* can reduce the size and unsteadiness of the ground vortex *without modification of the aircraft*, and without reduction of its thrust.

Acknowledgments

This project was made possible through the support of NASA-Ames Award No. NAG 2 - 484, Supplement 2.

References

1. Stanley, C. W., Hood, W. E., "Maintenance Problem Associated with the Operation of the F402 (Pegasus) engine in the AV-8A (Harrier) Aircraft," *Proceedings, AIAA/NASA Ames V/STOL Conference*, Palo Alto, Calif., December 7-9, 1981.

2. Mitchell, K. (ed.), *Proceeding of the 1985 NASA Ames Research Center's Ground-Effects Workshop*, NASA Ames Research Center, Moffett Field, CA, NASA CP 2462, Aug. 1985.

3. Margason, R. (ed.), *1987 Ground Vortex Workshop*, NASA Ames Research Center, Moffett Field, CA, NASA CP 1008, April 1987.

4. White, K. C. (ed.), *Proceedings of the International Powered Lift Conference*, Society of Automotive Engineers, Warrendale, PA, SAE P-203, Dec. 1987.

5. *SAE Aerospace Technology Conference and Exposition*, Society of Automotive Engineers, Warrendale, PA, Sept. 1989.

6. Cimbala, J. M., Billet, M. L., Gaublomme, D. P., and Oefelein, J. C., "Experiments on the Unsteadiness Associated with a Ground Vortex," *Journal of Aircraft*, Vol. 28, Number 4, April 1991, pp. 261-267.

7. Gaublomme, D. P., "Experiments on the Unsteady Ground Vortex," Masters Thesis, Department of Aerospace Engineering, Pennsylvania State University, August 1990.

8. Harman, T. B., "Reduction in Size and Unsteadiness of a V/STOL Ground Vortex by Ground Fences," Masters Thesis, Department of Mechanical Engineering, Pennsylvania State University, May 1992.

List of Figures

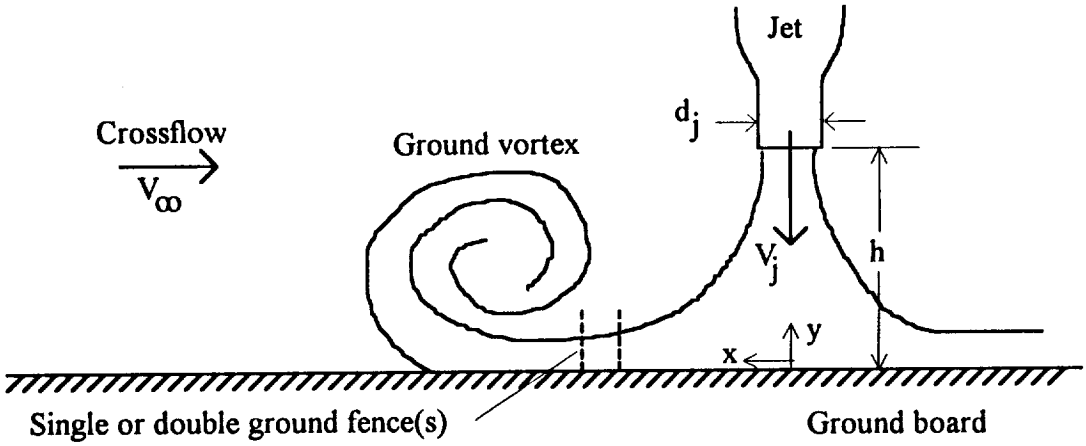

Figure 1 (Harman, Cimbala)

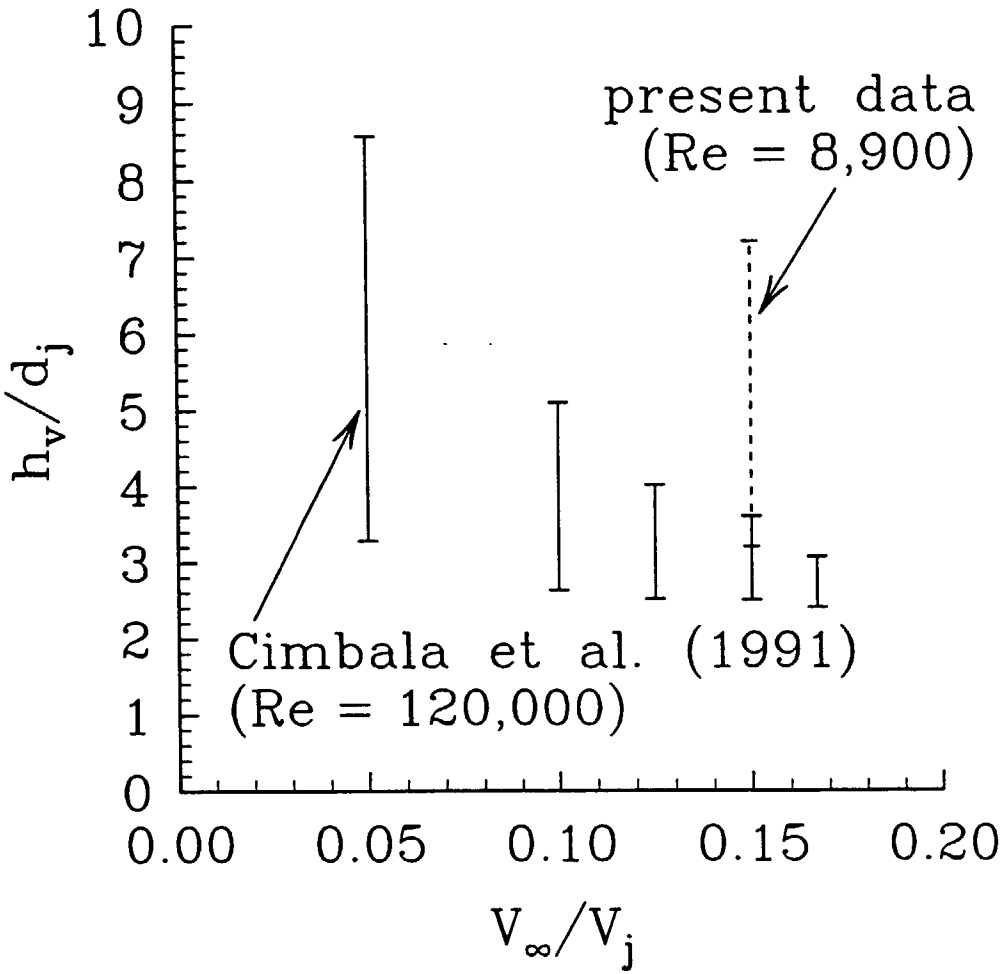

Figure 2 (Harman, Cimbala)

a)

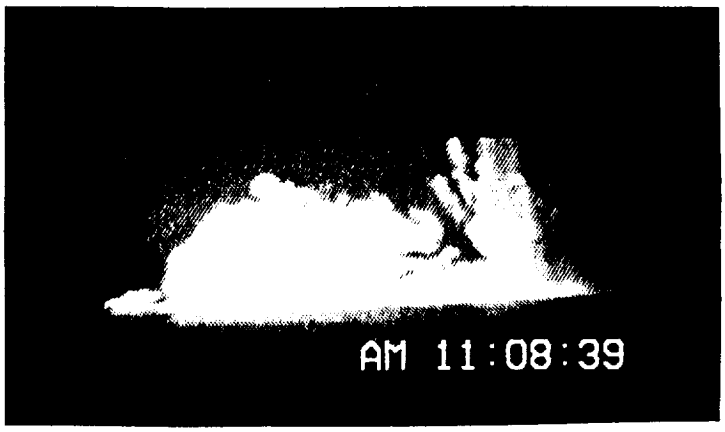

b)

Figure 3. (Harman and Cimbala)

a)

b)

c)

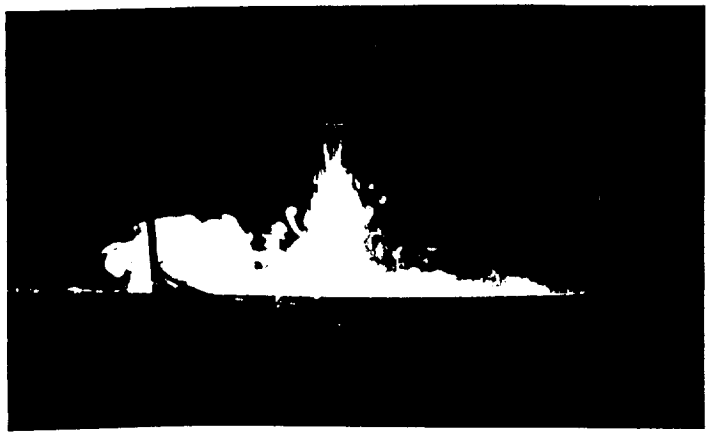

Figure 4. (Harman and Cimbala)

a)

b)

c)

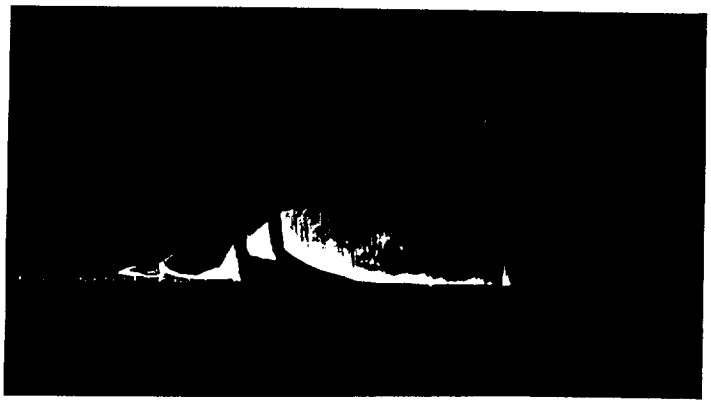

Figure 5. (Harman and Cimbala)

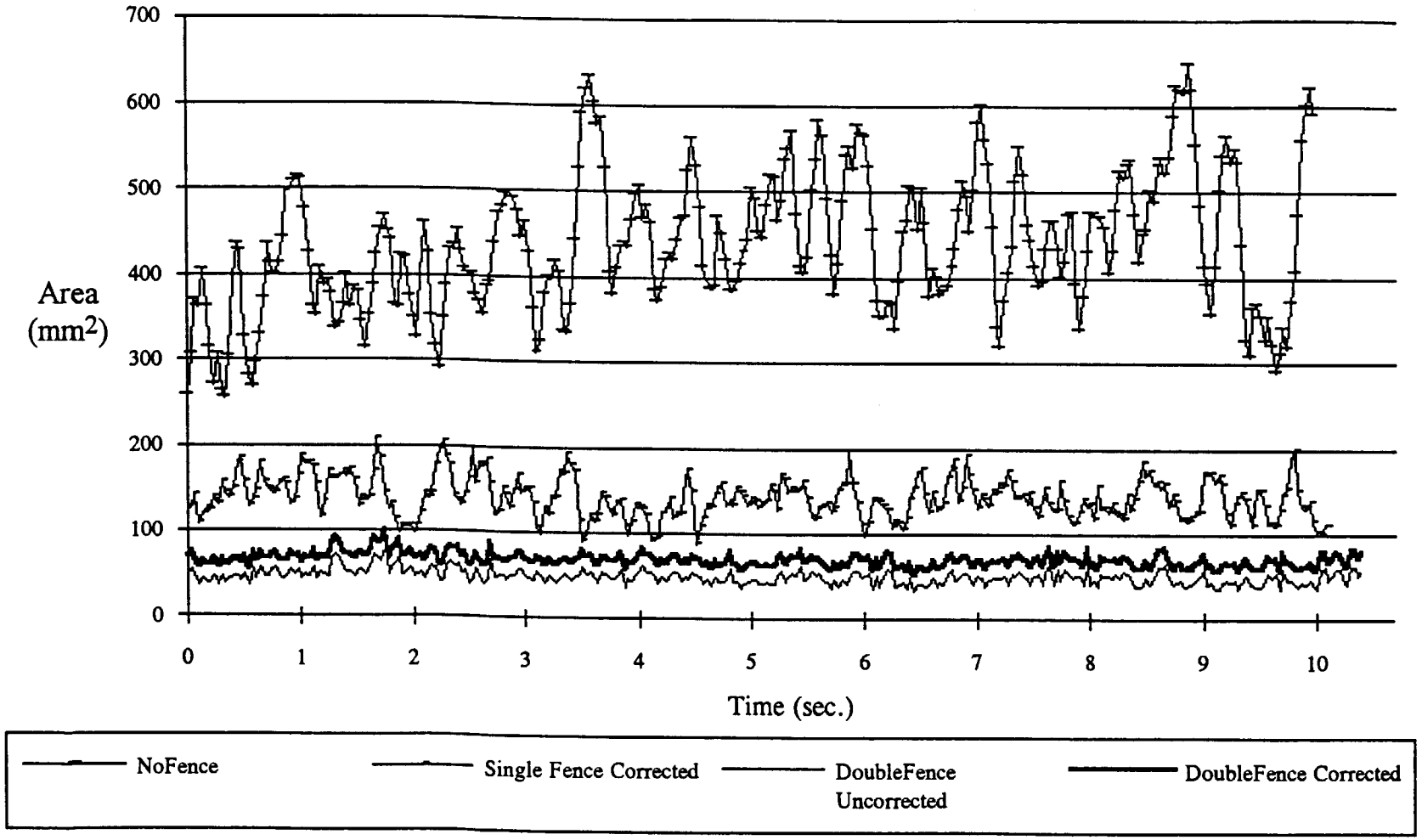

Figure 6. (Harman and Cimbala)

a)

Maximum mean size, no fence

Minimum mean size, no fence

b)

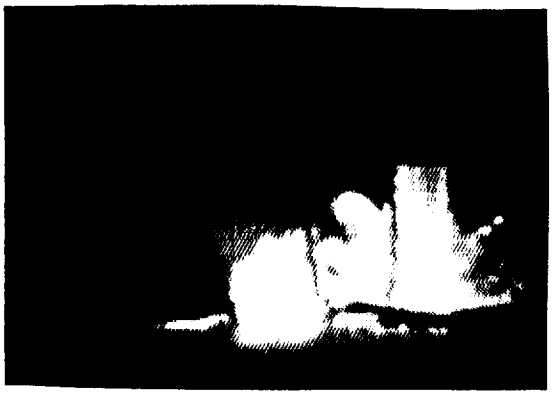

Maximum mean size, single fence

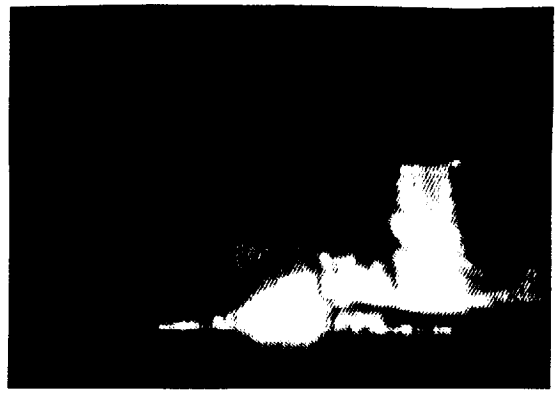

Minimum mean size, single fence

c)

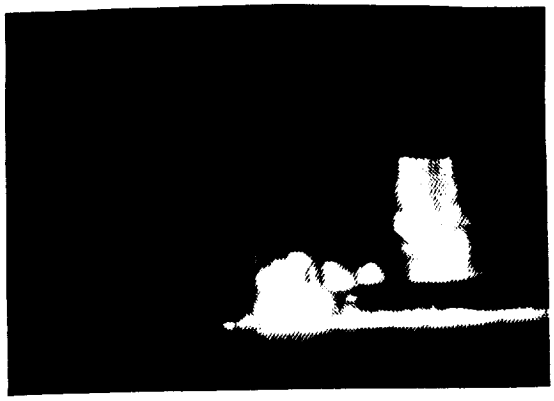

Maximum mean size, double fence

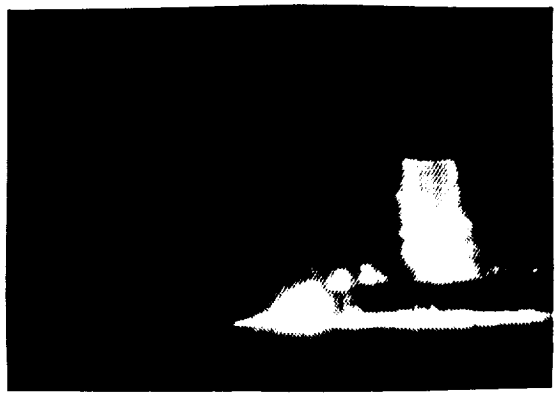

Minimum mean size, double fence

Figure 7. (Harman and Cimbala)

a)

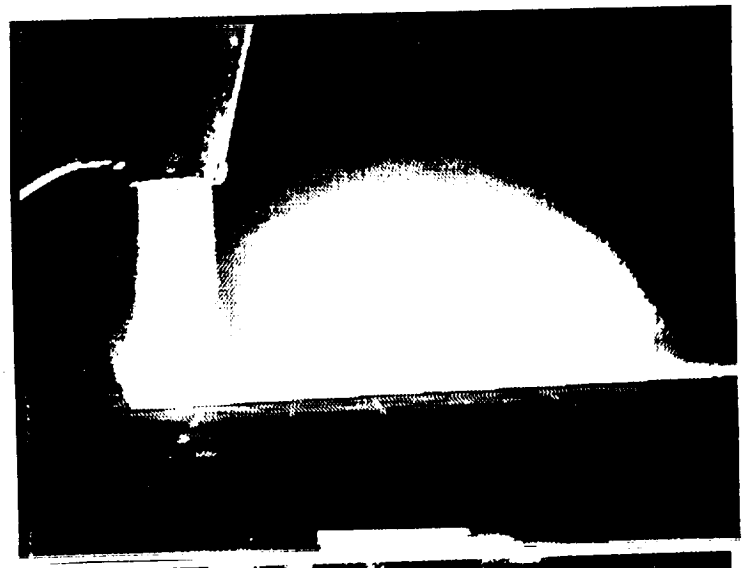

b)

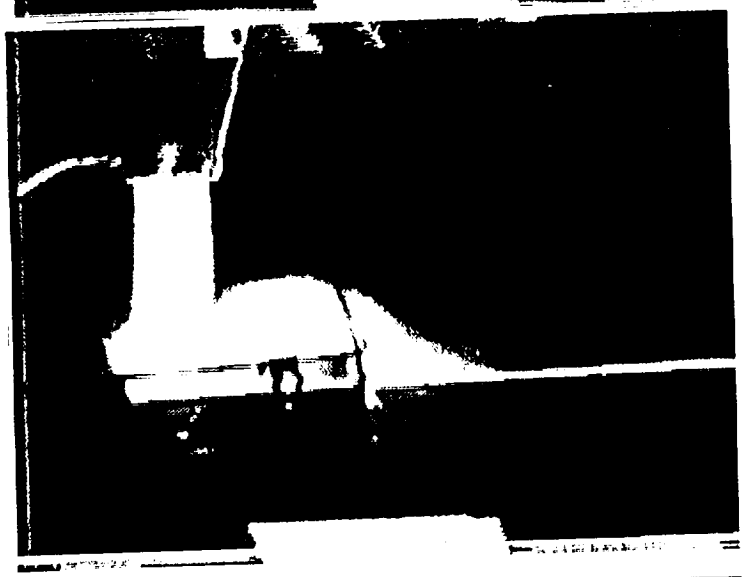

c)

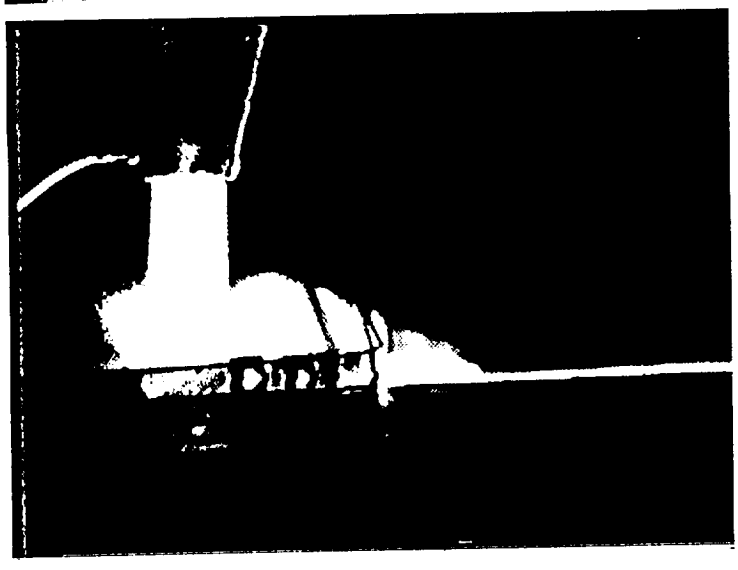

Figure 8. (Harman and Cimbala)